

NMR Characterization of Half-integer Quadrupolar Nuclei in Solids

J. P. Amoureux

Laboratoire de Dynamique et Structure des Matériaux Moléculaires (C.N.R.S.: U.R.A. 801),
Université des Sciences et Technologies de Lille, 59655 Villeneuve d'Ascq Cedex, France

Z. Naturforsch. **47a**, 665–674 (1992); revised version received February 5, 1992

This article describes a few aspects of NMR characterization of half-integer quadrupolar nuclei in powder samples which are either static or rotating around one fixed axis (M.A.S. and V.A.S. techniques). The simultaneous occurrence of C.S.A. and quadrupole interactions with possible non-coincident tensors is discussed.

Two experimental limitations are taken into account: the sample spinning speed and the RF-amplifier power.

Physics Abstract code numbers: 0758, 3240, 3325, 6116N, 7430G, 7660G.

I. Introduction

The main purpose of Nuclear Magnetic Resonance is the characterization of materials. One peculiar advantage of NMR with respect to other spectroscopies is that in this technique the analyses can be performed on each type of non-zero spin nucleus with three different complexity levels:

- determination of the different species with their respective proportions,
- determination of the physico-chemical surroundings of each species: chemical binding, C.S.A (Chemical Shift Anisotropy) and electric field gradients (quadrupolar interactions),
- determination of the dynamics of each species (chemical exchange).

This characterization is very easy to perform for liquids. Indeed, all interactions are then averaged by the Brownian motions and therefore yield very narrow lines.

This is not the case in solids in which very strong interactions always subsist. These interactions entail featureless broad bands with very small amplitudes which thus are usually embedded in the background noise. For this reason solid state NMR spectra were difficult to observe for a long time, until very high

magnetic field spectrometers became commercially available. At present, nearly all non-zero spin nuclei are observable in the solid state. For half-integer quadrupolar nuclei, several techniques are available either to narrow the spectra (M.A.S., V.A.S., D.O.R., and D.A.S.) or to facilitate the separation of the different species: two-dimension nutation experiments. The latter technique can also be used simultaneously with M.A.S., V.A.S. and D.O.R. Spectra observed with these different techniques mainly depend on the various interactions occurring in the sample. They may also be greatly distorted by numerous experimental spectrometer limitations.

In this article we will focus our attention on the one-dimension spectra observed in powder samples which are either static or rotating around one fixed axis (M.A.S. and V.A.S.). Indeed these kinds of experiments are, at present, the main interest of most NMR spectroscopists. We will consider on half-integer spins the two most important interactions in solids: the C.S.A. and quadrupolar interactions. We will also show that the spectrum lineshapes may be greatly changed by the C.S.A. even when this interaction is much smaller than the quadrupolar one. In this case, the relative orientations of both (C.S.A. and quadrupolar) P.A.S. (Principal Axes System) are always of prime importance. We will take into account two experimental limitations: the sample spinning speed and the R.F. amplifier power.

We will not discuss the spectrum distortions related to the dynamic aspects of nuclei (chemical exchange).

Reprint requests to Prof. J. P. Amoureux, Laboratoire de Dynamique et Structure des Matériaux Moléculaires (CNRS: URA 801), Université des Sciences et Technologies de Lille, F-59655 Villeneuve d'Ascq Cedex, France.

0932-0784 / 92 / 0500-0665 \$ 01.30/0. – Please order a reprint rather than making your own copy



Dieses Werk wurde im Jahr 2013 vom Verlag Zeitschrift für Naturforschung in Zusammenarbeit mit der Max-Planck-Gesellschaft zur Förderung der Wissenschaften e.V. digitalisiert und unter folgender Lizenz veröffentlicht: Creative Commons Namensnennung-Keine Bearbeitung 3.0 Deutschland Lizenz.

Zum 01.01.2015 ist eine Anpassung der Lizenzbedingungen (Entfall der Creative Commons Lizenzbedingung „Keine Bearbeitung“) beabsichtigt, um eine Nachnutzung auch im Rahmen zukünftiger wissenschaftlicher Nutzungsformen zu ermöglichen.

This work has been digitalized and published in 2013 by Verlag Zeitschrift für Naturforschung in cooperation with the Max Planck Society for the Advancement of Science under a Creative Commons Attribution-NoDerivs 3.0 Germany License.

On 01.01.2015 it is planned to change the License Conditions (the removal of the Creative Commons License condition “no derivative works”). This is to allow reuse in the area of future scientific usage.

II. R.F.-pulse Effects of Half-integer Quadrupolar Nuclei [1–4]

For nuclei with spin $I > 1/2$, the electric quadrupolar interaction is nearly always much stronger than the dipolar and C.S.A. interactions. The spin system comportment during the R.F. pulse can then be described by considering only the magnetic fields (\mathbf{B}_0 : static, \mathbf{B}_1 : rotating) and the quadrupolar interaction. In the laboratory frame, this interaction can be described in a first-order perturbation theory with the parameter

$$\bar{\omega}_Q = \frac{3C_Q}{8I(2I-1)} [3 \cos^2 \beta_s - 1 + \eta_Q \sin^2 \beta_s \cos 2\alpha_s]. \quad (1)$$

C_Q is the quadrupole constant, $0 \leq \eta_Q \leq 1$, the quadrupolar asymmetry parameter and (α_s, β_s) the polar angles describing \mathbf{B}_0 with respect to the quadrupolar P.A.S.

In a single-pulse experiment, a \mathbf{B}_1 R.F. magnetic field (amplitude and duration: ω_1 and t_1) is first applied along the ox' axis of the rotating frame. The F.I.D., which is to the 1st order calculation non zero only along oy' , is next recorded during the time t following this R.F.-pulse.

This transient depends only on the ratio between the two interactions considered during this pulse: $y = |\bar{\omega}_Q|/\omega_1$.

By summing up the signals corresponding to the two symmetrical transitions ($m, m-1$) and $(1-m, -m)$, this transient can be written

$$\begin{aligned} \text{Sy}'(\bar{\omega}_Q, t) = \sum_{m=1/2}^I \left\{ \cos[(2m-1)\bar{\omega}_Q t] \right. \\ \cdot \sum_q \text{ABS}_q^m(y) \sin[\omega_1 t_1 f_q(y)] + \sin[(2m-1)\bar{\omega}_Q t] \\ \cdot \left. \sum_q \text{DIS}_q^m(y) \cos[\omega_1 t_1 f_q(y)] \right\} \quad (3) \end{aligned}$$

with $(\forall m, y)$

$$\sum_q \text{DIS}_q^m(y) = 0, \quad (4)$$

$$\sum_q f_q(y) \text{ABS}_q^m(y) = (2 - \delta_{m1/2}) K_m. \quad (5)$$

$\delta_{m1/2}$ is the Kronecker notation and K_m the intensity of the $(m, m-1)$ or $(1-m, -m)$ symmetrical satellite transitions:

$$K_m = K_{1-m} = 1.5 \frac{I(I+1) - m(m-1)}{I(I+1)(2I+1)}. \quad (6)$$

The number of f_q nutation frequencies is $(I + 1/2)^2$. Equation (3) has been obtained with a first-order perturbation calculation and therefore its resonance frequency is zero for the central transition.

In a one-dimension experiment, spectra are deduced from $\text{Sy}'(\bar{\omega}_Q, t)$ with a Fourier-transform according to t . The first and second terms of (3) then correspond to absorption and dispersion signals, respectively. These dispersion terms, which are zero for the central transition, always remain very small (4), for the satellite transitions with the short R.F.-pulses normally used in this kind of experiment. Therefore we shall neglect them in the following.

In a two-dimensional nutation experiment, a second Fourier-transform according to t_1 is afterwards carried out. The first and second terms of (3) also correspond in this second dimension to absorption and dispersion signals, respectively. The two-dimension nutation spectra of satellite transitions are thus an absorption-dispersion mixture, even in the case of static samples.

III. Static Powder Samples

For static powder samples, two important effects have to be taken into account: the limited power of the R.F.-amplifier and the simultaneous occurrence of several interactions.

1. R.F.-Pulse Effects

In a powder sample, the quadrupolar interactions vary according to the crystallite orientation $(\alpha_s, \beta_s, (1))$. The R.F. magnetic field effects on the spin system may thus be different from a simple overall rotation around \mathbf{B}_1 of all individual crystallite magnetizations. A spectrum distortion may then arise from the R.F.-pulse application.

When satellite transitions are observed on a static sample, this involves a weak quadrupolar interaction which can then be neglected during the R.F.-pulse. As a result, the flip-angle corresponding to the maximum signal is slightly smaller than $\pi/2$ and the R.F.-pulse distortions are then negligible.

On the contrary, most of the time only the central transition is observed and the quadrupolar interaction is much stronger than the R.F. magnetic field. In order not to distort the spectra, it is then recommended to use very small flip-angles:

$$\omega_1 t_1 \leq \frac{2\pi}{3(2I+1)}. \quad (7)$$

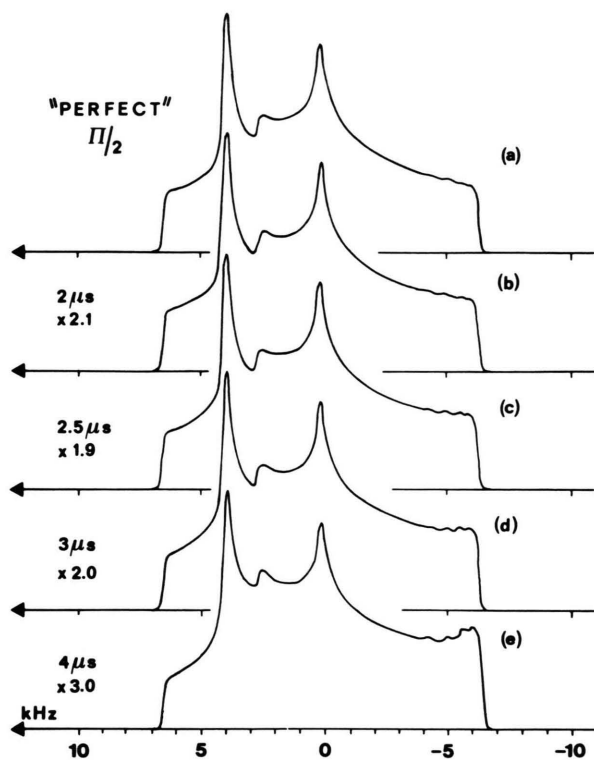


Fig. 1. Simulation of several central transition spectra of static powder samples according to the flip-angle. The ^{23}Na ($I=3/2$) quadrupolar parameters are those of Na_2SO_4 : $C_Q=2.6$ MHz and $\eta_Q=0.6$ [13]. The Larmor frequency is 105.6 MHz, the R.F.-magnetic field amplitude is 50 kHz ($\pi/2 \equiv 5 \mu\text{s}$) and the Gaussian broadening is 200 Hz (FWHM). The maximum amplitudes being identical for all spectra, the maximum signal ($\times 1.9$) is observed for a pulse duration of 2.5 μs : 45° flip-angle. The “perfect” $\pi/2$ pulse corresponds to an infinite amplifier power.

We have simulated (Fig. 1) several central transition powder spectra according to the flip-angle. We have always used the same experimental specifications (R.F. magnetic field amplitude: $\omega_1/2\pi = 50$ kHz ($\pi/2 \equiv 5 \mu\text{s}$), Larmor frequency: $\nu_0 = 105.6$ MHz) and ^{23}Na quadrupolar parameters ($I=3/2$, $C_Q = 2.6$ MHz) corresponding to Na_2SO_4 ($\eta_Q = 0.6$: Figs. 1, 3, 4, 5, 6, 8 a, 9) or Na_2MoO_4 ($\eta_Q = 0$: Figs. 8 b and c).

The maximum signal is observed for a $\pi/4$ flip-angle and the spectrum distortions are then very small. Thus we can conclude that in general the optimum flip-angle is determined by the Rabi law:

$$\omega_1 t_1 \cong \frac{\pi}{2I+1}. \quad (8)$$

In the particular case when all sample species are “a priori” submitted to weak quadrupolar interactions, the researcher may then apply greater flip-angles (slightly lower than $\pi/2$) in order to increase the S/N ratio.

In both cases, it is highly recommended to analyse “a posteriori” the spectra by taking into account the small distortions related to the R.F.-pulse effects.

2. Simultaneous Interactions

Nuclei with spin $I > 1/2$ are submitted to several different interactions: scalar and dipolar couplings, C.S.A. and quadrupolar interactions.

Scalar couplings are small and nearly unobservable on static powder samples.

Heteronuclear dipolar couplings with “strong” nuclei (^1H , ^{19}F , ^{31}P , ...) may be cancelled by using usual decoupling techniques.

Homomuclear dipolar couplings are always weak and quasi-isotropic and they can be satisfactorily described with a phenomenological Lorentzian/Gaussian broadening.

Thus, two main anisotropic interactions are only to be taken into account in solids: C.S.A. and quadrupolar interactions.

According to whether the quadrupolar interaction is strong or weak, the static powder spectra of half-integer quadrupolar nuclei are then, “convoluted” by the C.S.A., only the central or all transitions, respectively. For a powder sample experiment C.S.A. and quadrupolar tensors are individually defined by 3 and 2 parameters, respectively. The simultaneous description of both interactions generally requires 8 parameters “a priori”. Three Euler angles (α_σ , β_σ , γ_σ) are indeed necessary to define the C.S.A. tensor with respect to the quadrupolar P.A.S.

Most of the time, in order to decrease by 3 the number of unknown parameters, both P.A.S. interactions are assumed identical, even when not required from the lattice site symmetry. Obviously, the simulation of experimental spectra may sometimes be very difficult within this hypothesis.

A detailed characterization of quadrupolar nuclei in the solid state, with the definition of the 8 previous parameters for each species, is however possible. This detailed analysis, usually performed with a single-crystal, can be reached with a powder sample if several independent experimental data are available: different static magnetic fields and samples either static

or rotating with several spinning speeds. Following this increasing scientific interest in simultaneous interactions, several groups [5–8] have very recently described the static powder spectra of quadrupolar and C.S.A. non-coincident interaction tensors.

We first analysed the ^{133}Cs spectra of cesium chromate (Cs_2CrO_4). There are two crystallographically distinct cesium sites in the unit cell, each located on a mirror plane. A single-crystal NMR study [9] has recently established the quadrupolar and chemical shielding parameters for the two cesium nuclei and also indicated that at both sites, the two tensors are non-coincident in the mirror plane. The two P.A.S. are deduced from each other by a rotation around the direction perpendicular to the mirror (Euler angles $(0, \beta_\sigma, 0)$). The ^{133}Cs nuclei ($I=7/2$) having a relatively small quadrupole moment and a moderate chemical shift range, their powder spectra reflect all transitions. The static powder spectra corresponding to site no. 2 (according to Power et al. [8]) is shown in Figure 2. It can be observed on this figure that the introduction of C.S.A. onto the quadrupolar pattern gives a much more complicated spectrum. The small quadrupolar interaction leads to spectral overlap of the central transition by the satellites. The effect of varying the relative orientations of the quadrupolar and C.S.A. tensors are illustrated by changing the β_σ angle.

When the quadrupolar interaction is strong enough, only the central transition is observed. The resulting spectrum is then a “convolution” of the quadrupolar (2nd order) and C.S.A. (1st order) interactions. The important effects of varying the relative orientations

$(0, \beta_\sigma, 0)$ of both tensors are illustrated in Fig. 3 by changing the β_σ angle between the two P.A.S.

IV. Rotating Powder Samples

1. Generalities

From the lattice site symmetry, non-coincident tensors have usually to be considered. These relative P.A.S. orientations can be expressed with respect to either the quadrupolar or the C.S.A. tensors. In both cases, the powder lineshapes are obviously identical. However, it is much easier to orient the C.S.A. tensor into the quadrupolar P.A.S. when considering second-order quadrupolar effects for the central transition.

Let us first consider a single-crystal rotating with ω_R angular frequency about an axis θ tilted from \mathbf{B}_0 . The spin system description needs three successive changes of frame. The first one ($\alpha_\sigma, \beta_\sigma, \gamma_\sigma$) connects the C.S.A. to the quadrupolar P.A.S., the second (α, β, γ) the quadrupolar P.A.S. to the rotor and the third ($\omega_R t, \theta, 0$) the rotor and laboratory frames.

The instantaneous resonance corresponding to the $(m, m-1)$ transition is then given by

$$\omega_{m, m-1}(t) = \omega_m + \omega_R \sum_{n=1}^4 n \{ \bar{A}_n^m \cos n(\omega_R t + \gamma) + \bar{B}_n^m \sin n(\omega_R t + \gamma) \} \quad (9)$$

with

$$\bar{A}_n^m = \bar{A}_{n1}^\sigma + \bar{A}_{n1}^{mQ} + \bar{A}_{n2}^{mQ}; \quad \bar{B}_n^m = \bar{B}_{n1}^\sigma + \bar{B}_{n1}^{mQ} + \bar{B}_{n2}^{mQ}. \quad (10)$$

Equations (9) and (10) correspond to perturbation theories, either to the first-order for C.A.S. (\bar{A}_{n1}^σ and

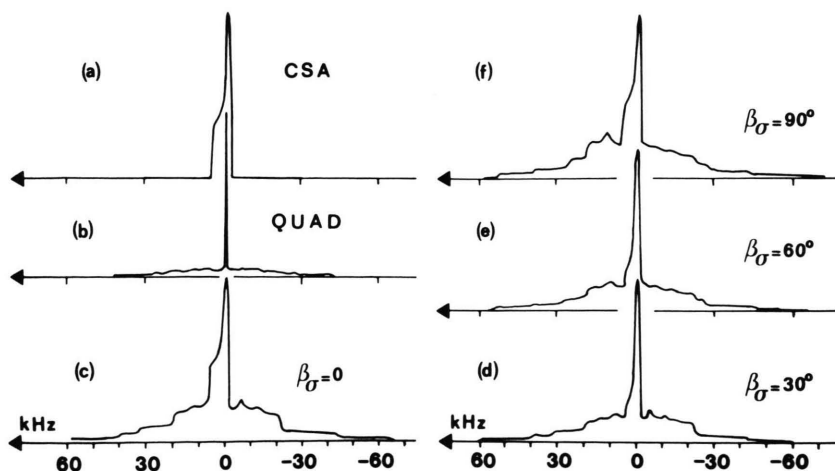


Fig. 2. Simulation of static powder sample spectra corresponding to small quadrupole and C.S.A. interactions. The ^{133}Cs ($I=7/2$) quadrupolar and chemical parameters are those of Cs_2CrO_4 : $C_Q=0.373$ MHz, $\eta_Q=0.55$ and $\Delta\sigma=270$ ppm, $\eta_\sigma=0.293$ ([8], site 2). The Larmor frequency is 26.247 MHz. Figures 2a and b correspond to C.S.A. or quadrupolar interaction, respectively, Figs. 2c–f correspond to C.S.A. and quadrupolar interactions, with different $(0, \beta_\sigma, 0)$ relative orientations.

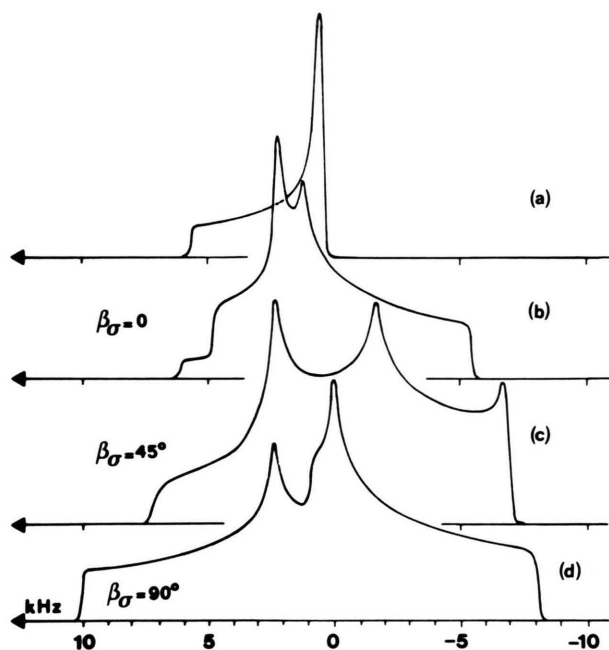


Fig. 3. Simulation of central transition spectra of static powder samples submitted to simultaneous interactions. Larmor frequency, quadrupolar parameters and broadening are those of Figure 1. Chemical shielding parameters are $\Delta\sigma = 50$ ppm and $\eta_\sigma = 0$. Figures 3a and 1a correspond to C.S.A. or quadrupolar interactions, respectively. Figures 3b, c, d correspond to C.S.A. and quadrupolar interactions, with different $(0, \beta_\sigma, 0)$ relative orientations.

\bar{B}_{n1}^σ) or to the second-order for quadrupolar interaction (1st order: \bar{A}_{n1}^{mQ} and \bar{B}_{n1}^{mQ} ; 2nd order: \bar{A}_{n2}^{mQ} and \bar{B}_{n2}^{mQ}).

The $\omega_R \bar{A}_{n1}^\sigma$ terms depend on the $\alpha, \beta, \alpha_\sigma, \beta_\sigma, \gamma_\sigma$, and θ angles and on the C.S.A. interaction ($\Delta\sigma$: amplitude; $0 \leq \eta_\sigma < 1$: asymmetry parameter). The $\omega_R \bar{A}_{n1}^{mQ}$ terms depend on the $(m, m-1)$ transition, on the α, β , and θ angles, on the Larmor frequency (2nd order) and on the quadrupolar interaction (C_Q, η_Q). The same dependences hold for the $\omega_R \bar{B}_{n1}^{mQ}$ and $\omega_R \bar{B}_{n1}^\sigma$ terms.

ω_m is the time-independent resonance, including the isotropic chemical shift, observed with a sample which is either static or rotating with an “infinite” ω_R spinning speed. Its value depends on all previous parameters and angles.

2. Sideband Intensities

A single-crystal spectrum is composed of rotational sidelines appearing every ω_R . The signal, including

R.F.-pulse effects, corresponding to the $(m, m-1)$ transition can then be expanded into a Fourier series:

$$S(m, t, \alpha, \beta, \gamma) = K_m \text{RF}(m, \alpha, \beta, \gamma) \sum_{N=-\infty}^{\infty} H(m, N, \alpha, \beta, \gamma) \cdot \exp i \{ \omega_m(\alpha, \beta) + N \omega_R \} t \quad (11)$$

with, (3),

$$\text{RF}(m, \alpha, \beta, \gamma) = \sum_q \text{ABS}_q^m \sin [\omega_1 t_1 f_q], \quad (12)$$

$$H(m, N, \alpha, \beta, \gamma)$$

$$= \frac{1}{2\pi} F(m, N, \alpha, \beta, -\gamma) \int_{-\pi}^{\pi} du F^*(m, N, \alpha, \beta, u), \quad (13)$$

and

$$F(m, N, \alpha, \beta, u) = \exp i \left\{ -Nu + \sum_{n=1}^4 (\bar{A}_n^m \sin nu + \bar{B}_n^m \cos nu) \right\}. \quad (14)$$

The H functions are complex and the sideline pattern corresponding to a rotating single-crystal is thus an absorption-dispersion mixture [10].

Most of the experiments are performed with powder samples and the signal is then obtained by averaging (11) over all (α, β, γ) crystallite orientations.

It is advisable to perform first this average over the Euler angle γ which only appears in the H and RF functions:

$$S(m, t, \alpha, \beta) = \frac{K_m}{2\pi} \sum_N \exp i(\omega_m + N \omega_R) t \cdot \int_{-\pi}^{\pi} d\gamma \text{RF}(m, \alpha, \beta, \gamma) H(m, N, \alpha, \beta, \gamma). \quad (15)$$

3. Non-selective R.F.-pulse Effects on Rotating Powder Samples

When the R.F.-pulse has either a very short t_1 duration or an ω_1 amplitude much higher than the C.S.A. and quadrupolar interactions, the latter can be neglected during the pulse which is then called “non-selective”. In this case, the R.F.-pulse effect corresponds for all individual magnetizations to a simple rotation around \mathbf{B}_1 of an angle $\omega_1 t_1$:

$$S(m, t, \alpha, \beta) = K_m \sin(\omega_1 t_1) \sum_N H(m, N, \alpha, \beta) \cdot \exp i \{ \omega_m(\alpha, \beta) + N \omega_R \} t \quad (16)$$

with

$$H(m, N, \alpha, \beta) = \frac{1}{4\pi^2} \left| \int_{-\pi}^{\pi} du F(m, N, \alpha, \beta, u) \right|^2. \quad (17)$$

This $H(m, N, \alpha, \beta)$ function being real positive, the spectrum of each rotating “super-crystal” (only defined by the (α, β) polar angles) is then only an absorption signal. Obviously, this characteristic remains true for rotating powder samples [11].

4. Selective R.F.-pulse Effects on Rotating Powder Samples

When the R.F.-pulse is too long and too weak, its effects vary according to the Euler angle γ from one “super-crystal” to another and the integral of (15) cannot be simplified as (17). The sideband amplitudes are complex and the rotating powder spectra are then “a priori” an absorption-dispersion mixture.

However, the dispersion signal always remains small in a one-dimension experiment, especially if the quadrupolar interaction is not very strong. Moreover, this signal is cancelled when the R.F.-pulse is short enough, when the rotation speed is sufficient (no spinning sideband) or when $\eta_Q = 0$ or 1.

Furthermore, for realistic R.F.-pulses, this small dispersion signal (when it exists) can always be phase-corrected with the absorption; its origin being approximately at mid-pulse.

This dispersion term has then only to be taken into account in two dimension nutation experiments when spinning sidebands appear on the spectra and when η_Q is different from 0 and 1.

5. M.A.S.: R.F.-pulse Effects

In order to analyse the R.F.-pulse effects in the M.A.S. condition ($\theta_m = 54.736^\circ$) we have chosen the central transition of Na_2SO_4 .

When the rotation speed is not sufficient, numerous sidebands appear on the spectra (Fig. 4). Experimental and simulated spectra are quasi-identical (Figs. 4a and b). The total spectrum (absorption + dispersion) is greatly distorted only for large flip-angles (Figure 4d).

When the spinning speed is quasi-sufficient, few sidebands appear on the spectra (Fig. 5). The agreement between experimental and simulated spectra is nearly perfect (Figs. 5a and b). The total spectrum distortions remain reasonable (Fig. 5c) even for a $\pi/2$ flip angle.

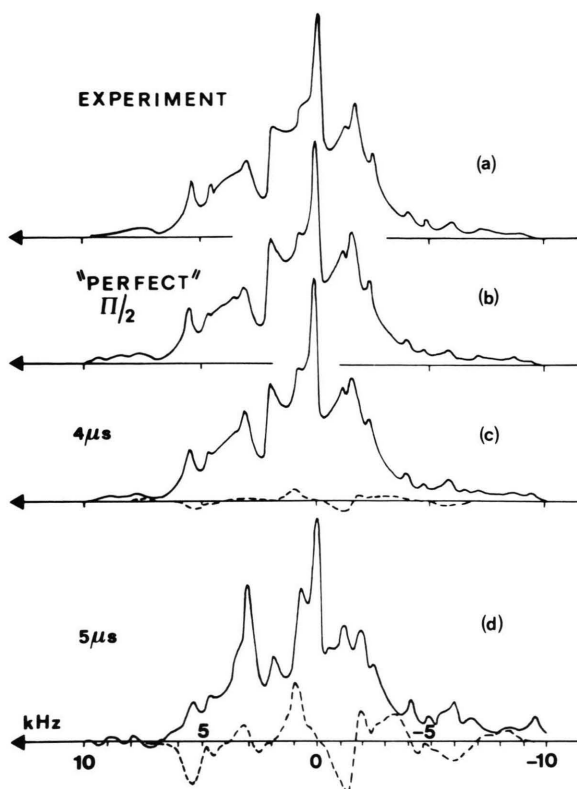


Fig. 4. Central transition spectra of Na_2SO_4 powder samples for a slow M.A.S. spinning speed 2350 Hz. Larmor frequency, R.F.-magnetic field amplitude, quadrupolar parameters and broadening are those of Figure 1. Continuous and dashed curves correspond to absorption and dispersion signals (along oy'), respectively. The dispersion signal and the distortions are important only for the $\pi/2$ flip-angle (Figure 4d).

We may then conclude that in usual one-dimension NMR experiments, the dispersion signal along oy' always remains negligible, even with a slow rotor spinning speed.

6. M.A.S.: Non-coincident Interaction Tensors

C.S.A. interactions are always very weak with respect to the Zeeman interaction and thus can be treated with a 1st order perturbation theory. In the M.A.S. condition, their effects then disappear from the spectra if the rotation speed is sufficient: no spinning sideband. If this is not the case, C.S.A. interactions are “observable” either on the central transition pattern or on all spinning sidebands of satellite transitions, according to whether quadrupolar interactions are strong or not.

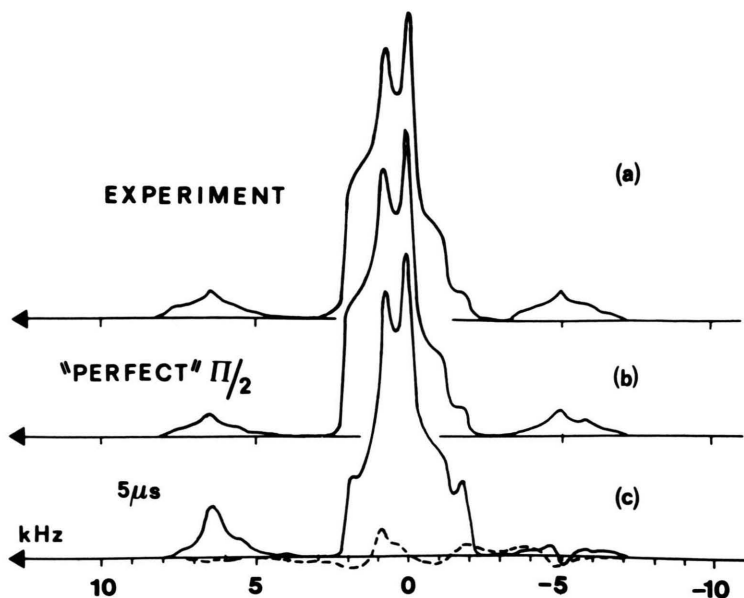


Fig. 5. Central transition M.A.S. spectra of Na_2SO_4 powder samples for a relatively fast spinning speed 5690 Hz. Larmor frequency, R.F.-magnetic field amplitude, quadrupolar parameters and broadening are those of Figure 1. Continuous and dashed curves correspond to absorption and dispersion signals (along oy'), respectively. The dispersion signal and the distortions remain very small even for a $\frac{\pi}{2}$ flip-angle (Figure 5c).

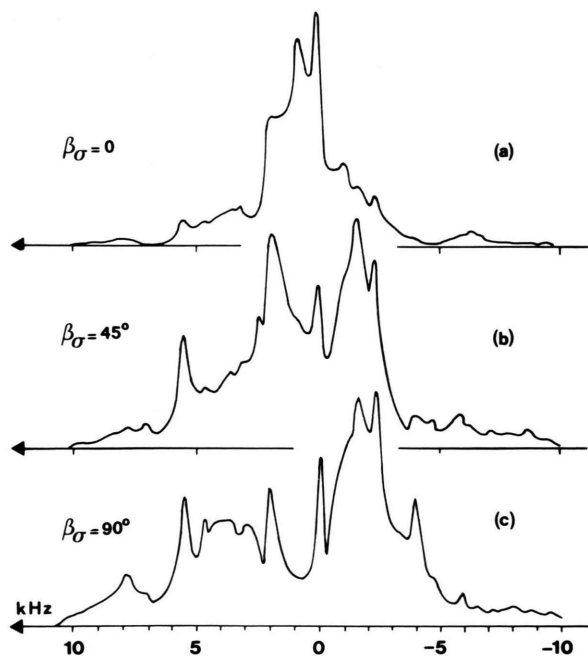


Fig. 6. Simulation of central transition spectra submitted to simultaneous interactions for a slow M.A.S. spinning speed 2350 Hz. Larmor frequency, quadrupolar parameters and broadening are those of Figure 1. Chemical shielding parameters are $\Delta\sigma = 50$ ppm and $\eta_\sigma = 0$ and the relative P.A.S. orientations are $(0, \beta_\sigma, 0)$. These figures have to be compared with Figure 4b.

We have displayed (Fig. 6) several M.A.S. central transition spectra in the case of a slow spinning speed. These spectra have been simulated by adding to the “strong” ^{23}Na quadrupolar interaction of Na_2SO_4 a small C.S.A. interaction ($\Delta\sigma = 50$ ppm, $\eta_\sigma = 0$) with various relative P.A.S. orientations $(0, \beta_\sigma, 0)$. One can observe (Figs. 4b and 6) that a very small amount of C.S.A. may completely change the central transition spectra corresponding to “strong” quadrupolar interactions, if the spinning speed is not sufficient. This effect may certainly explain the small differences (in the 0–2 kHz frequency range) observed between Figs. 4a and b.

We have analysed the ^{133}Cs M.A.S. spinning sideband pattern of cesium chromate. The quadrupolar and chemical shielding parameters for both sites are those determined by the single-crystal NMR study [9]. Spinning sideband integrated intensities have been calculated either for the quadrupolar interaction only (Fig. 7b) or for C.S.A. simultaneously (Figs. 7c, d, e). In the latter cases the relative P.A.S. orientations $(0, \beta_\sigma, 0)$ for both sites have been varied. The best agreement with the experimental [8] integrated intensities (Fig. 7a) is obtained (without refinement) for relative P.A.S. orientations deduced from a single crystal NMR experiment (Figure 7d).

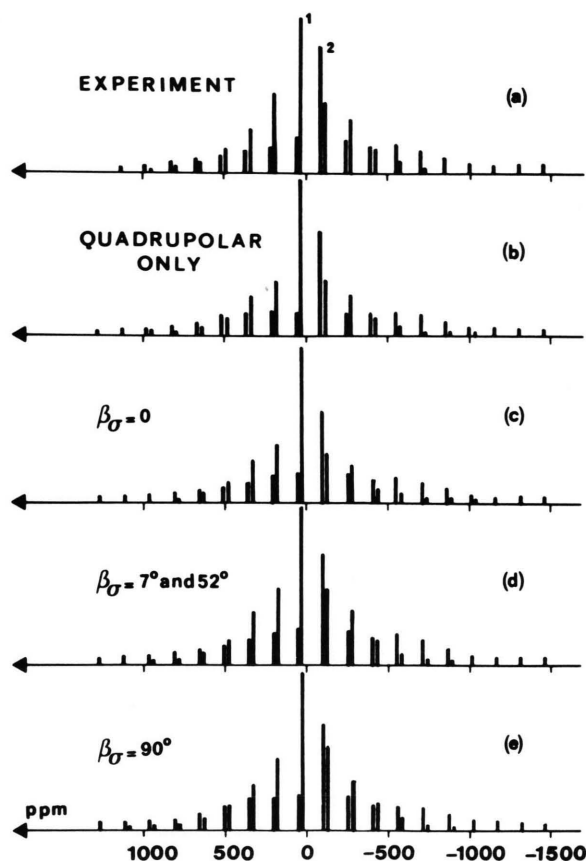


Fig. 7. ^{133}Cs integrated intensities of Cs_2CrO_4 in the M.A.S. condition. Larmor frequency and quadrupolar and chemical shielding parameters for site 2 are those of Figure 2. For site 1, these parameters are [8]: $C_Q = 0.142$ MHz, $\eta_Q = 0.11$ and $\Delta\sigma = -333$ ppm, $\eta_\sigma = 0.041$, $\nu_R = 4000$ Hz. The experimental integrated intensities have been evaluated from Fig. 5 of [8]. The relative tensor orientations $(0, \beta_\sigma, 0)$ are: $\beta_{\sigma 1} = \beta_{\sigma 2} = 0$ (Fig. 7c), $\beta_{\sigma 1} = 52^\circ$, $\beta_{\sigma 2} = 7^\circ$ (Fig. 7d) and $\beta_{\sigma 1} = \beta_{\sigma 2} = 90^\circ$ (Fig. 7e).

7. V.A.S.: Powder Sample Spectra

Sample rotation at the magic angle θ_m is at present the major technique used to narrow the powder spectra. However it is possible, "a priori", to narrow further the central transition spectra by spinning the rotor about another axis: V.A.S. (Variable Angle Spinning) technique. The maximum narrowing is observed for a θ angle of about 65° [12–14]. This extra narrowing is visible on Figs. 4b and 8, where the ^{23}Na central transition spectra corresponding to the "strong" quadrupolar interactions of Na_2SO_4 and Na_2MoO_4 are simulated for a slow spinning speed. Since the spectrum linewidths are approximately divided by 2

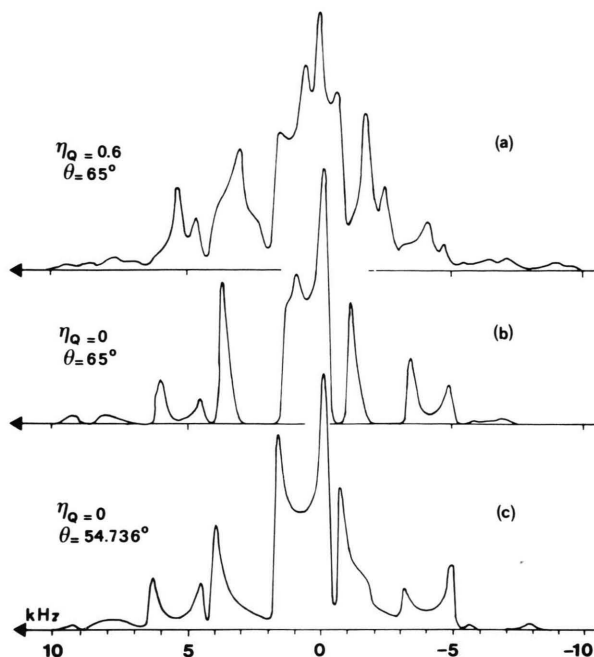


Fig. 8. Simulation of central transition spectra corresponding to a slow spinning speed (2350 Hz) and a strong quadrupolar interaction. Larmor frequency, quadrupolar constant and broadening are those of Figure 1. The η_Q asymmetry parameter is 0.6 (Fig. 8a) or 0 (Figs. 8b and c). The θ rotation angle is 65° (Figs. 8a and b) or 54.736° (Fig. 8c). Figures 4a and 8a and Figs. 8b and c have to be compared.

when θ is increased from θ_m to 65° , the sideband intensities are much smaller for $\theta = 65^\circ$ (Figs. 8a and b) than for the magic angle (Figs. 4b and 8c). Unfortunately, Figs. 8a and b have been simulated by taking into account only quadrupolar interactions. In reality, other weak interactions (C.S.A. and dipolar couplings) exist which are only zeroed in the M.A.S. condition. Therefore, the experimental spectra observed at $\theta = 65^\circ$ are often wider than at the magic angle.

Moreover the simulation of the featureless V.A.S. spectra is much more complicated than in the M.A.S. condition because more unknown parameters are needed. For these reasons, most NMR spectroscopists always use the M.A.S. technique even for half-integer quadrupolar nuclei.

The only rare case in which the V.A.S. technique has to be preferred is when the C.S.A. and dipolar interactions are negligible with respect to the quadrupolar central-transition width.

Thus, the real use for the V.A.S. technique is in the D.A.S. (Dynamic Angle Spinning) experiments [15, 16]

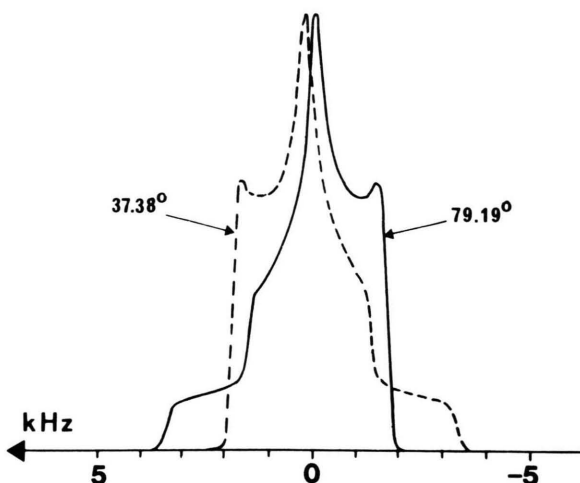


Fig. 9 Simulated central transition spectra corresponding to a fast spinning speed. Larmor frequency, quadrupolar parameters and broadening are those of Figure 1. Spectra corresponding to both θ rotation angles (37.38° and 79.19°) are symmetrical to each other.

which are derived from it. These D.A.S. experiments allow all different interactions to be cancelled at least up to the 2nd order. In its simplest description a D.A.S. experiment corresponds to the juxtaposition of two consecutive FIDs, with identical τ duration, recorded at the θ angles 37.38° and 79.19° .

These two rotational angles correspond to reverse spectra for all 1st and 2nd order interactions (Fig. 9) and the spin system refocuses at time 2τ . The central transition spectra of powder samples are then only composed of thin lines only broadened by residual 3rd (C.S.A. and dipolar couplings) and 4th order (quadrupolar) interactions.

V. Conclusions

After analysing the R.F.-pulse effects on powder sample spectra, we have shown that in a one-dimension NMR experiment, the R.F.-pulse distortions can easily be avoided with sufficiently short pulses. Their optimal duration for the central transition is nearly always determined by the Rabi law: $\omega_1 t_1 = \pi/(2I + 1)$. For this flip angle the distortions are very small and the S/N ratio is nearly always maximum.

These R.F.-pulse effects are used in the 2-dimensional nutation technique. However, the analysis of these 2-dimension spectra must take into account the

dispersion signals for the satellite transitions (in all cases) and for the central transition of rotating powder samples (if the spinning speed is not sufficient and if η_Q is different from 0 and 1).

We have also analysed the effects related to the simultaneous existence of C.S.A. and quadrupolar interactions. These effects may arise "a priori" when the chemical shielding range is of the same order as the transition linewidth considered.

However, in the M.A.S. condition the C.S.A. influences the spectra only when the spinning speed is not sufficient. In this case the lineshapes are changed by a weak C.S.A. interaction and the experimental spectra may not be simulable in the framework of exclusive quadrupolar interactions.

The two P.A.S. corresponding to these interactions may also be non-coincident and up to 8 parameters are then required to characterize each species properly. It is then compulsory to increase the number of independent experimental data to access these numerous unknown parameters: experiments performed with different Larmor frequencies with sample either static or rotating with several spinning speeds.

In addition to the two previous experimental limitations (R.F.-amplifier power and spinning speed), many other experimental contingencies have also to be taken into account:

- the spectrometer bandwidth, mainly determined by the coil features and the sampling antialiasing filter,
- the Lorentzian/Gaussian broadening which represents the residual dipolar interactions, the usual exponential multiplication and the magnetic field inhomogeneity,
- the electronic dead-time,
- the more or less well performed linear phase-correction,
- the baseline correction,
- the pulse repetition delay between two successive accumulations which may be too short with respect to the "recovery times" of all species,
- the spinning speed fluctuations which mainly broaden the thin outermost sidebands,
- the possible distribution of parameters arising from non-uniform surroundings in partially crystallised compounds (e.g., zeolites).

Analytically, taking into account all these contingencies is obviously impossible. The only solution to characterize solid materials correctly is to use a computer simulation program [17–19].

Acknowledgements

The author would like to thank Doctors C. Fernandez, L. Carpentier, and E. Cochon for their decisive

help in the development of this work. He is also very grateful to Professors H. Jacobsen and coworkers, J. B. Nagy, E. G. Derouane, and Doctor F. Lefebvre for the very helpful discussions he had with them.

- [1] A. Samoson and E. Lippmaa, *J. Magn. Reson.* **79**, 255 (1988).
- [2] P. P. Man, *J. Magn. Reson.* **67**, 78 (1986).
- [3] V. D. Mijden, R. Janssen, and W. S. Veeman, *Mol. Phys.* **69**, 53 (1990).
- [4] L. Carpentier, Thesis, University Lille 1990.
- [5] P. J. Chu and B. C. Gerstein, *J. Chem. Phys.* **91**, 2081 (1989).
- [6] J. T. Cheng, J. C. Edwards, and P. D. Ellis, *J. Phys. Chem.* **94**, 553 (1990).
- [7] P. W. France, *J. Magn. Reson.* **92**, 30 (1991).
- [8] W. P. Power, R. E. Wasylshen, S. Mooibroek, B. A. Pettitt, and W. Danchura, *J. Phys. Chem.* **94**, 591 (1990).
- [9] S. Mooibroek, Ph.D. Thesis, Dalhousie University 1987.
- [10] M. M. Maricq and J. S. Waugh, *J. Chem. Phys.* **70**, 3300 (1979).
- [11] M. H. Levitt, *J. Magn. Reson.* **82**, 427 (1989).
- [12] F. Lefebvre, J. P. Amoureux, C. Fernandez, and E. G. Derouane, *J. Chem. Phys.* **86**, 6070 (1987).
- [13] S. Ganapathy, S. Schramm, and E. Oldfield, *J. Chem. Phys.* **77**, 4360 (1982).
- [14] S. Ganapathy, J. Shore, and E. Oldfield, *Chem. Phys. Lett.* **169**, 301 (1990).
- [15] A. Llor and J. Virlet, *Chem. Phys. Lett.* **152**, 248 (1988).
- [16] K. T. Mueller, Y. Wu, B. F. Chmelka, J. Stebbins, and A. Pines, *J. Amer. Chem. Soc.* **113**, 32 (1991).
- [17] J. P. Amoureux, C. Fernandez, and L. Carpentier, Bruker report 2, 1990.
- [18] J. P. Amoureux, C. Fernandez, L. Carpentier, and E. Cochon, *Mol. Phys.* (1992), in publication.
- [19] J. Skibsted, N. C. Nielsen, H. Bildsoe, and H. Jakobsen, *J. Magn. Reson.* **95**, 88 (1991).